



Geospatial analyses of oceanographic and atmospheric parameters off the California coast

Jason Adelaars, California State University of Monterey Bay

Mentor: Dr. Leslie Rosenfeld

Summer 2012

Keywords: SST, chlorophyll, wind, currents, geospatial, MPA monitoring

ABSTRACT

Remotely-sensed ocean observing technologies and numerical models have generated years of spatiotemporal data for the purposes of visualizing, understanding, and forecasting marine conditions. Many products based on these data can be accessed on the Central and Northern California Ocean Observing System website. Users are able to view maps of various parameters in order to observe past, present, or near future conditions of the ocean. However these products are somewhat limited in their capacity for calculating geospatial statistics. Having the ability to perform spatial and temporal analyses of the ocean's physical parameters could have broad applications for marine researchers and policy-makers. Therefore, the purpose of this project was to convert historical sea surface temperature, ocean color (proxy for chlorophyll concentration), currents, and wind datasets into formats that can be executable with geospatial software. Furthermore, several examples of analyses that can be performed with these data are presented. The results of this project will improve marine stakeholder's understanding of the physical components in the dynamic marine environment through geospatial data analysis and visualization.

INTRODUCTION

There is somewhat of a data rift between two fundamental regimes of marine research efforts. Traditionally, studies in physical oceanography require a background in physics to understand fluid dynamics and energy fluxes inherent in oceanographic conditions. Moreover, these studies often involve time-series datasets of broad spatial extents, requiring computing power and programming knowledge in order to manipulate the data and acquire results (Schwarz et al. 2010, Kim 2009). On the other hand, studies of marine ecology are often temporally static or occur on annual frequencies (Anderson et al. 2009, MacCall and Prager 1988). Ecological studies are also heavily dependent on high spatial accuracy, due to the fine spatial scales required to evaluate species-environment interaction (Young et al. 2010). The latter efforts of marine research are becoming more frequently used and understood by marine management and stakeholders (Leslie and McLeod 2007, Crowder and Norse 2008). However, an understanding of the physical parameters is somewhat elusive to those outside of oceanographic research. Bringing oceanographic observational datasets into the spatial analysis realm could help bridge this rift and improve marine management decisions.

Ocean observing systems provide useful tools for visualizing the physical components of the dynamic marine environment across broad spatial scales. Remote-sensing techniques, such as satellite imaging and high-frequency (HF) radar, are capable of producing daily to hourly distributions of oceanographic conditions (NASA 2011, Kim et al. 2007). This includes sea surface temperature (SST), ocean color, and current vectors. Furthermore, data-assimilating oceanographic and atmospheric numerical models allow for the nowcast, and even forecast, of oceanic and atmospheric conditions (Shulman et al. 2002). The results can be downloaded for use in scientific research or displayed on map layouts to characterize the distribution of each physical parameter.

These products and others have enhanced marine research capabilities in describing the physical dynamics that drive ecosystem variability. In the California Current System (CSS), where marine organismal community dynamics are greatly influenced by coastal upwelling of deep sea nutrients, studies have incorporated ocean observing data to explain trends in ecological parameters. For example, Kahru et al. (in

press) incorporated data from historical in situ observations and satellite measurements to plot chlorophyll concentration time series for several regions within the CCS. The results indicated a trend of increasing chlorophyll concentrations off the central and southern coast of California, paired with decreasing concentrations near Baja California and within the North Pacific gyre. Kim (2010) used HF radar to observe spatial and temporal variability in eddies offshore of southern California. His study demonstrated the utility of HF radar-derived currents as a complement to satellite remote sensing observations, for understanding coastal dynamics.

Traditionally, research of these time series variables have been conducted by groups with the computing power of technical and specialized software, such as MATLAB®. This software provides users with the capability of calculating statistics over time and space to yield results. However, these datasets are typically in binary or array formats, which creates difficulty for users not trained to manipulate those types of data. Consequently, most ecologists and marine managers, who generally lack a background in physics and programming, have limited access to such data resources. This somewhat hinders the incorporation of dynamic variables into the scope of marine ecology and policy.

To reconcile this disconnect, the purpose of this project was to convert several oceanographic datasets (SST, chlorophyll, current, wind) into formats that can be read and analyzed by geospatial software; with the intent for these to be hosted by CeNCOOS. Furthermore, several analyses were demonstrated to understand the capabilities of these geospatial data. The goal of this project was to examine whether dynamic parameters could be displayed and analyzed with geospatial software. The results of this project could open up new capabilities for marine research analytics, as well as provide marine managers with additional information on which to base decisions.

MATERIALS AND METHODS

To achieve the goals of this project, multiple datasets of various temporal and spatial resolutions were converted into a format that could be opened and manipulated with geospatial software. Upon retrieval from their respective sources, each dataset was formatted to execute in MATLAB, which was the primary processing software of

CeNCOOS. The final data format desired by this project was ARC GRID raster, which has been the common raster format of ArcMap (ESRI 2011). Raster data are structured as a geographically referenced grid containing measurements. Grid cell width and length dictate the resolution of the data. The ARC GRID format was chosen for this project due to the growing use of ArcMap as a geospatial analyst and visualization tool. Therefore, MATLAB (v2012a, The MathWorks) and ArcMap (v10.0, ESRI) were the primary data conversion tools during used during this project. A general workflow of each dataset's conversion is provided in Appendix A.

DATA SOURCES AND CONVERSION

Sea surface temperature and chlorophyll

Sea surface temperature (SST) observations were made by the National Oceanic and Atmospheric Administration's (NOAA) Polar-orbiting Operational Environmental Spacecraft (POES). Two satellites (NOAA-17 and NOAA-18) equipped with Advanced Very High Resolution Radiometers (AVHRR) provide multiple daily radiance images. Radiance is further processed into SST images using the non-linear sea surface temperature (NLSST) algorithm (Walton et al. 1998).

Ocean color (proxy for chlorophyll concentration) was measured by the Moderate Resolution Imaging Spectroradiometer (MODIS) mounted on the National Aeronautics and Space Administration's (NASA) Aqua Satellite. Chlorophyll-a concentrations are computed using the NASA-developed OC3M algorithm (O'Reilly et al. 2000).

These data were downloaded from the NOAA National Marine Fisheries Service Environmental Research Division Data Access Program (ERDDAP). The datasets consists of daily 3-day composited SST and chlorophyll observations from January 2008 through December 2011. The data were composited to reduce spatial gaps due to cloud cover. The spatial extent of the datasets used for this project were subsetted from a global extent to consist of only the entire length of California from the coastline seaward to the 126° W longitudinal line. When downloaded, the data come with an associated latitude/longitude reference grid. This grid has a 1.3-km resolution.

The data were downloaded in array format using a created MATLAB script. The observation files were associated with an existing coordinate grid and converted to ascii text format using the *arcgridwrite* function (<http://www.mathworks.com/matlabcentral/fileexchange/16176-arcgridwrite>). In ArcMap, the ascii files were converted into ARC GRID raster layers and projected into North American Datum 1983, California Teale-Albers (meters). This projection is commonly used for displaying data across a California-wide extent. The layers were clipped to the California coastline to eliminate measurements made from lakes.

Currents

Surface current vector components were collected from a network of HF radar shore stations along the western coast of the United States and processed by Sung Yong Kim (Scripps Institute of Oceanography). Processing consisted of gridding current vector components. The grid points missing data were filled using optimal interpolation which is dependent upon covariance matrices of the surrounding grid points (Kim et al. 2007 and Kim et al. 2008). This method optimally fills gaps within the dataset, caused by intermittent shutdowns of shore stations or inadequate algorithm solutions. Optimally interpolated gridded data creates spatially and statistically consistent datasets (Kim in prep).

The complete dataset consisted of hourly observations along the whole West Coast of the U.S. for the years of 2008 and 2009. The data off California were averaged into daily 3-day composites. This was done both to match the temporal frequency of the satellite datasets and to average over tidal variability. The grid cells had a spatial extent of 5.6-km longitudinally and 6-km latitudinally. The rectangular grid cells conflicted with the output formatting of an ascii text file, which require square cells. Therefore, the data were exported from MATLAB into geotiff format using the built-in *geotiffwrite* function in the Mapping Toolbox. Geotiff files are georeferenced tagged image files, which supports grids with rectangular cells. The *geotiffwrite* function requires an associated geographic reference file to accurately write the raster data into the correct spatial domain.

Once in ArcMap, the geotiff layers were copied into an ARC GRID format and projected to NAD 1983, California Teale-Albers (meters). The extent of the layers cover the length of California to approximately 150-200 km offshore.

Wind

The wind dataset was provided by the Naval Research Laboratory (NRL) in Monterey, California. The data were generated by the Coupled Ocean/Atmosphere Mesoscale Prediction System (COAMPS[®]) which produces 48-hour surface (~10m) wind forecasts every twelve hours. The dataset provided consisted of the twice daily nowcast and forecasts from April 2009 to May 2012. There were several instances of missing daily measurements within the dataset. In these cases, the forecast of the previous day were incorporated to fill those gaps. The nowcast observations were averaged into daily 3-day composites similarly to the averaged SST, chlorophyll, and current datasets. The vector components required rotating from the model coordinate system onto a true north coordinate system grid. The dataset came projected in an unknown coordinate system, which displayed the data in non-square grid cells. This created difficulty in converting the data to raster grids, because the *arcgridwrite* function prefers equal latitude/longitude grid spacing and *geotiffwrite* requires a referenced coordinate system. Therefore, the data were interpolated onto a square mesh grid and ASCII files were exported from MATLAB using the *arcgridwrite* function.

In ArcMap the layers were converted to ARC GRID format, clipped to the California coast, and reprojected to NAD 1983, California Teale-Albers (meters). The raster layers are 3.06-km resolution and cover the length of California from the coastline seaward to the 126° W longitude line.

Bathymetry and MPA boundaries

The time-series datasets were spatially analyzed based on the boundaries of existing marine protected areas (MPA) along the central and north central coast of California (figure 1). A polygon shapefile representing these MPAs was downloaded from the California Department of Fish and Game Marine GIS Unit's webpage (CDFG 2012). Thirteen MPAs were selected based on their size (>20km²) and adjacency to the

coastline. These selected MPAs were subsequently used to demonstrate several spatial analyses throughout the remainder of this report.

Sonar-derived bathymetry layers were used as a visual reference in the final figures (figures 1, 3, 4). These layers were downloaded from the websites of NOAA and CDFG (<http://www.ngdc.noaa.gov/mgg/bathymetry/multibeam.html>; <http://www.dfg.ca.gov/marine/gis/bathymetry.asp>).

ANALYSIS

The following analyses were conducted in an effort to demonstrate the utility of time-series spatial data. Monthly averages, used in several analyses, were calculated using every third day within each month, since the time-series used already consisted of 3-day composites or averages. Due to time constraints, wind and chlorophyll analyses were not incorporated during this project.

Cross/Along Shore Currents

To assess the cross-shore and along-shore water movement within MPAs, 3-4 of the current raster's grid cells nearest to each MPA or MPA pairing (State Marine Reserve and State Marine Conservation Area) within the central and north-central California coast were subsampled by selecting the chosen grid cells by their respective Field ID attribute. A blank raster layer (MPA key) was created from these subsampled grid cells as a spatial extent reference for further analysis outputs. The MPA key was converted into a point shapefile (Raster to Point) and copied (Copy Feature) several times for using later on in the analysis (*blank_mpa* shapefile). In order to express the velocity vector in terms of cross-shore and along-shore orthogonal components, reference lines were drawn in ArcMap to represent the coastline orientation along large segments of the coast (figure 1). Using an open-source tool, Easy Calculate 10, the azimuth (degrees clockwise from north) of each line was computed (Tchoukanski 2012). The azimuth was subsequently recalculated to equal the number of degrees counterclockwise from north. These values were appended onto the nearest MPA feature in the *blank_mpa* shapefile. This shapefile was then converted back into a raster grid (*angle_key*) with the same cell size and extent as the original current vector component rasters. The resulting values within the *angle_key* raster represented the angles used to rotate the current vector components.



Figure 1: Overview of central and north central coast MPAs (purple). Labeled MPAs were used in spatial analyses. Coastal orientation lines (orange) were drawn to represent overall orientation of the coastline for the cross/along shore current analysis. Bathymetry provided by California Department of Fish and Game (CDFG); terrestrial basemap provided by ESRI.

The vector (u and v) components were recomputed using the Raster Calculator according to the following calculations:

$$u_{rot} = u \times \cos(|angle_key| \times \frac{\pi}{180}) + (v \times \sin(|angle_key| \times \frac{\pi}{180}))$$

$v_{rot} = -u \times \sin(|angle_key| \times \frac{\pi}{180}) + (v \times \cos(|angle_key| \times \frac{\pi}{180}))$ where $angle_key$ is in degrees.

This computation effectively projects the velocity vector onto a coordinate system wherein v_{rot} is parallel to the reference coastline and positive towards the northwest, and u_{rot} is perpendicular to the coastline and positive towards shore. The components were averaged spatially (Zonal Statistics) and temporally (Cell Statistics) and plotted to identify trends.

SST

Monthly SST averages were computed using the Cell Statistics tool. From those temporal averages, spatial averages were calculated within each MPA (Zonal Statistics). An MPA shapefile was converted into a raster layer (*MPA_raster*) using the Polygon to Raster tool in the Conversion toolbox. The output raster's extent and cell size were set to be the same as a SST raster. Skipping this step would require the Zonal Statistics tool to do this operation for each iteration, increasing the computing time.

The results from the zonal statistics analysis of each monthly mean were appended onto the attribute table (Extract Multivalued to Point) of a *blank_mpa* point shapefile which was subsequently used to plot the time series of the monthly averages. A shapefile's database file can be opened in Microsoft Excel to create line graphs.

Find Fronts

Temperature fronts were identified using an open-source ArcGIS Toolbox called Marine Geospatial Ecology Tools (MGET) developed at Duke University (Roberts et al. 2010). A front can be defined as the thin region of separation between two bodies of constant temperature (Cayula and Cornillon 1992). MGET features a tool (Cayula-Cornillon Fronts in ArcGIS Raster) based on Cayula and Cornillon (1994) that identifies the boundaries between different water masses. The tool's algorithm searches for bimodal

frequency histograms within a moving window and flags the center cell when input arguments are met. This tool accepts a suite of input arguments:

- Temperature difference
- Window size
- Smoothing resolution
- Window stride
- Proportion of pixels with data
- Population size proportions
- Minimum criterion function (θ , Cayula and Cornillon 1994)
- Cohesion parameters

For the tool to run properly the input SST raster values must be integers. In order to conserve SST resolution to 0.1°C, the input raster was multiplied by 100 and then rounded to nearest integer. A number of different combinations of input argument values were tried in order to understand how each input argument affects the output image.

RESULTS

CONVERSION

In total, 1461 chlorophyll layers, 1461 SST layers, 721 u and v paired current vector layers, and 1126 u and v paired wind vector layers were created in ARC GRID raster format. Each layer is a 3-day composite of the target date and the complete days before and after. The raster layers are all projected to NAD 1983 California Teale-Albers (meters) and appear in their correct orientation when opened in ArcMap.

ANALYSIS

Cross/Along shore current

Temporal variability in cross-shore and along-shore currents within MPAs were consistent with existing knowledge of the coastal upwelling within the CCS. The monthly-averaged cross-shore and along-shore speeds near Point Sur ranged from 0 to 15 cm/s and 0 to 20 cm/s, respectively (figure 2). During the spring and summer months of 2008 and 2009, current ran in a relatively swift offshore and equatorward direction which

is consistent with coastal upwelling. For example, the monthly mean from March 2008 (figure 3) exhibited offshore and equatorward movement in 100% of the eleven 3-day composites, which comprised the monthly average. This can be associated with strong equatorward directed winds, favorable to coastal upwelling.

In the fall and winter, the current was weaker with some months exhibiting onshore and poleward flow. 55% and 22% of the 3-day averages in February 2009 (figure 4) exhibited offshore and equatorward movement, respectively. During the winter, winds are variable and often from the south, which contributes to this reversal in current direction. Variability within the month was observed to be greater in the along-shore current (standard deviation 5-15 cm/s) than in the cross-shore current (5-10 cm/s).

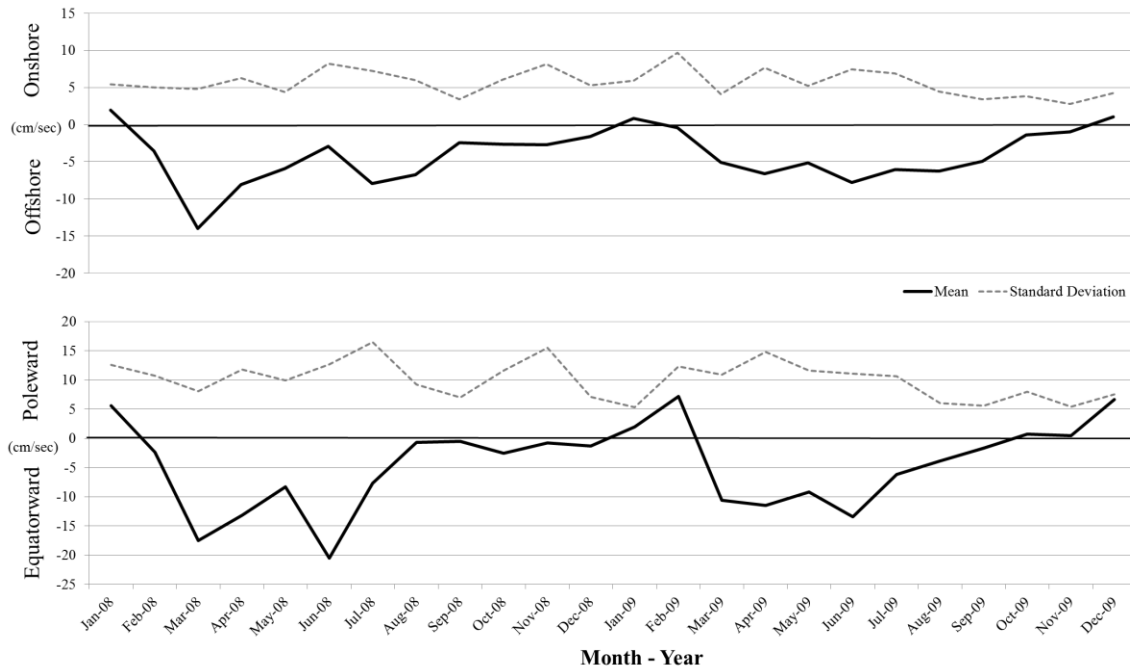


Figure 2: Monthly-averaged cross-shore (above) and along-shore (below) current spatially averaged over the area near the Point Sur MPA pairing (SMR and SMCA) are shown by the black solid lines. Standard deviations of the 3-day averaged currents within each month are shown by the grey dashed lines. The extreme months of March 2008 and February 2009 are highlighted in figures 3 and 4, respectively.

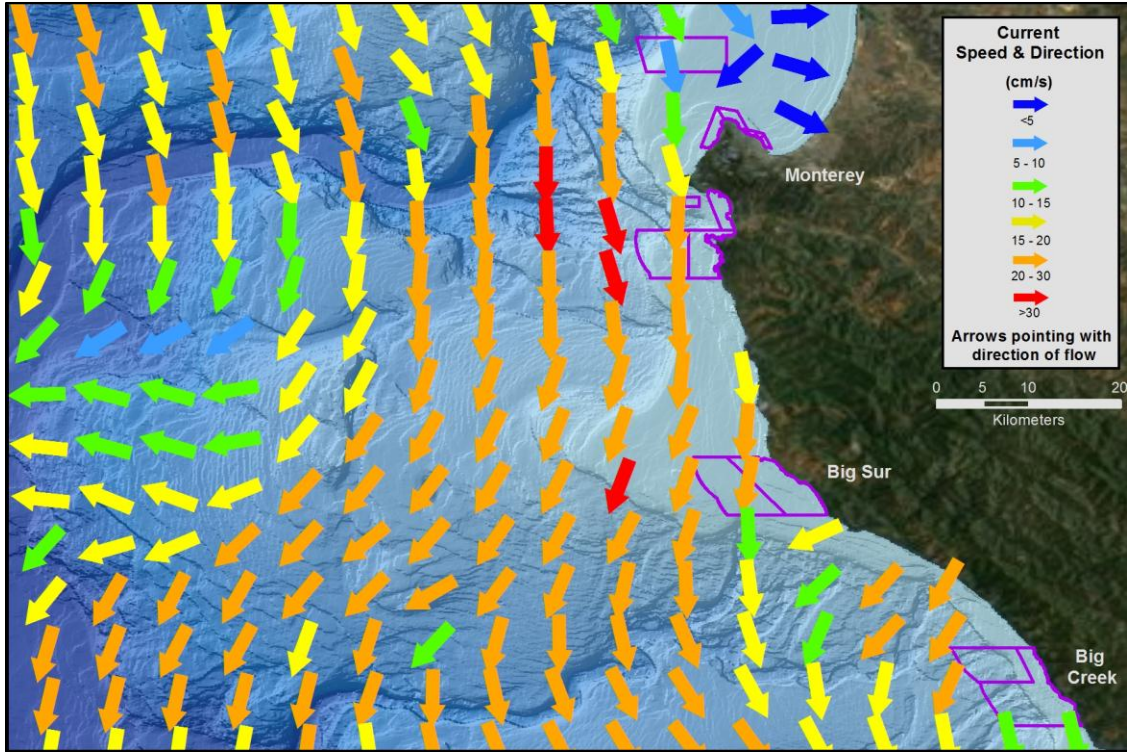


Figure 3: Mean current direction and magnitude for March 2008. MPAs depicted in purple.

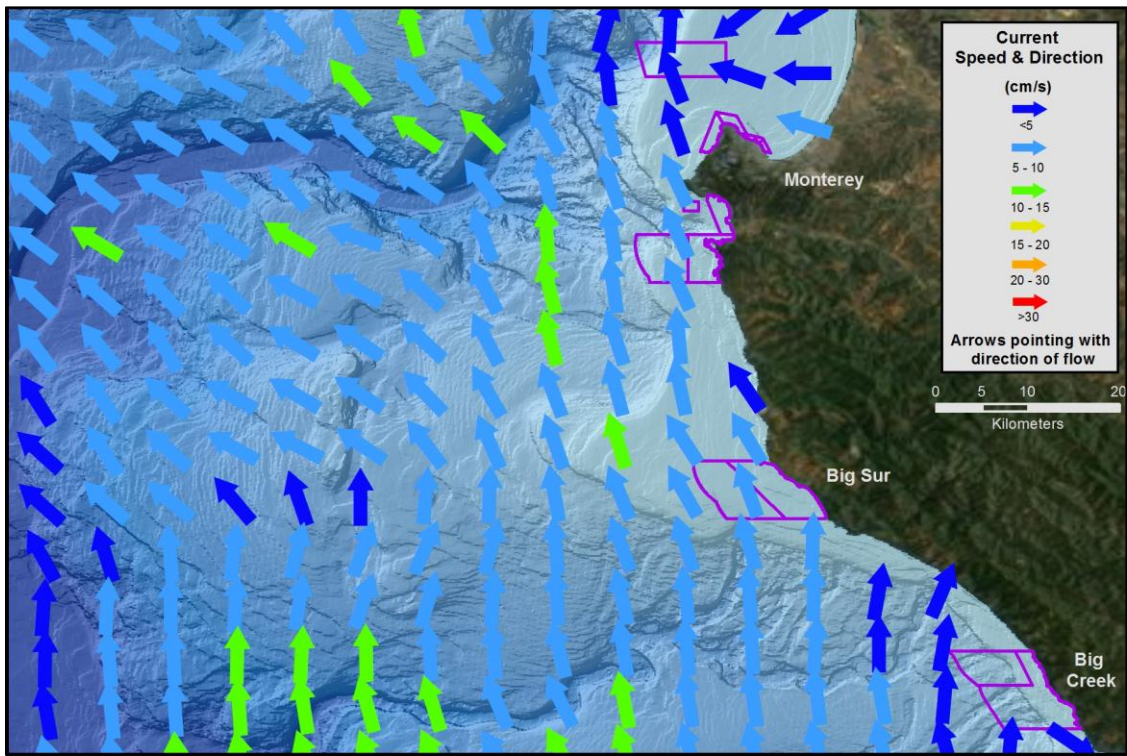


Figure 4: Mean current direction and magnitude for February 2009. MPAs depicted in purple.

Plotting the monthly averages of multiple MPA regions can provide understanding of larger spatial variations. Figure 5 represents the cross-shore and along-shore movement of water within 13 selected MPAs between Point Conception and Point Arena. Through 2008 and 2009, surface waters flowed predominantly offshore. Maximum annual offshore flow occurred in April for both years, whereas the minimum offshore flow was exhibited in February 2009. Temporal variation of along-shore flow resembles the variation for the Point Sur region depicted in figure 2. Equatorward maxima occurred in March 2008 and 2009 before gradually shifting poleward in the winter months.

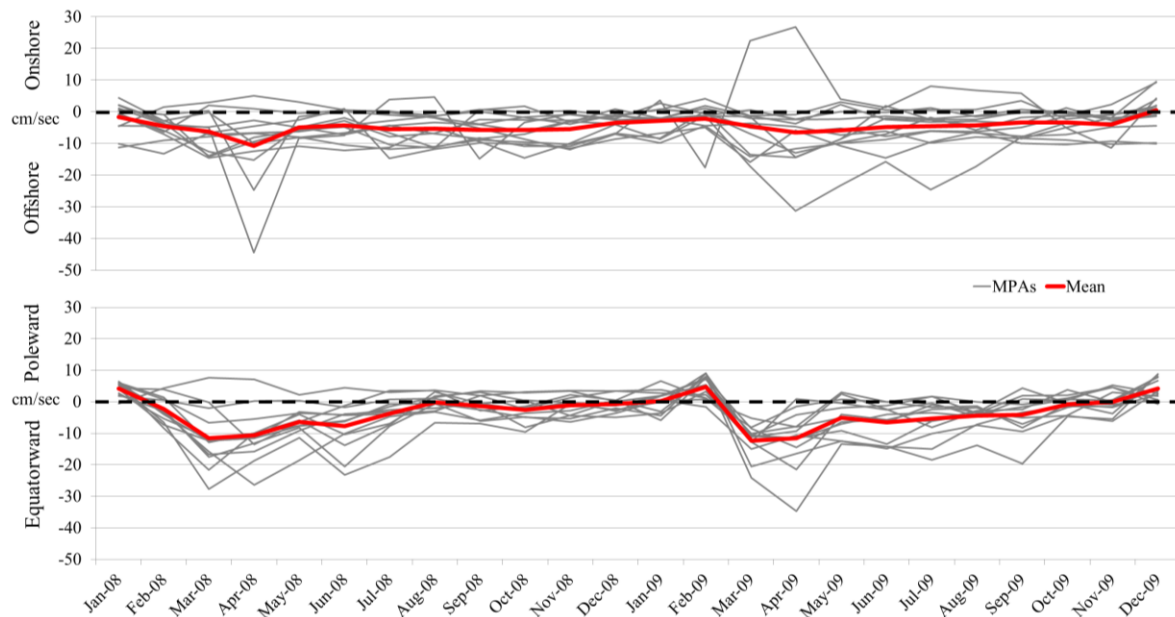


Figure 5: Monthly-averaged cross-shore (above) and along-shore (below) current spatially averaged over each of 13 MPA regions from Point Conception to Point Arena are shown by the grey lines. The average flow over all those MPA regions is represented by the red line.

SST

The results of this analysis were focused on selected MPAs. Figure 6 displays the spatially averaged monthly mean SST within the Point Lobos MPAs. Figure 7 displays the monthly mean SST of MPAs along a latitudinal gradient. This was done to demonstrate the method for both individual and multiple MPAs. Spatially averaged SST plots for MPAs along the entire California coast can be created with these data.

SST within the Point Lobos MPAs was observed to have annual fluctuations between approximately 11 and 15 degrees Celsius from 2008 through 2011. Annual lows were observed in April/May which is consistent with when coastal upwelling is generally strongest. The annual SST highs occurred in late summer, corresponding to the period of light winds and strong heat flux from the atmosphere.

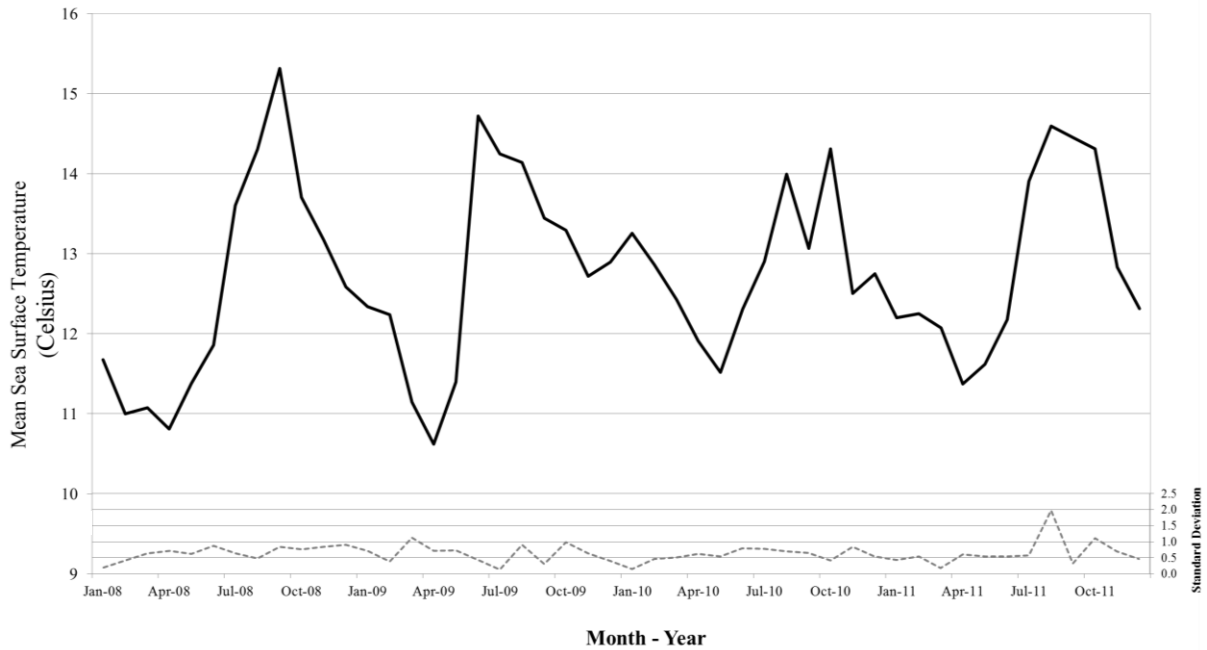


Figure 6: Monthly and spatially averaged SST (degrees Celsius) within the Point Lobos MPA pair (SMR and SMCA) from 2008 through 2011.

Figure 7 displays SST for selected MPAs along the central and north-central California coast. The Cambria MPA was excluded from this analysis due to its small size and lack of associated SST datapoints. Therefore, only 12 MPAs were examined in this analysis. As expected the lower latitude MPAs were observed to have warmer temperatures than their higher latitude counterparts. The general pattern of annual fluctuations of sea surface temperature between the late-summer maxima and early-spring minima is observed in all the MPA areas. The calculated latitudinal temperature difference of the MPAs ranges between 1.3 and 4.9°C throughout the 4-year period.

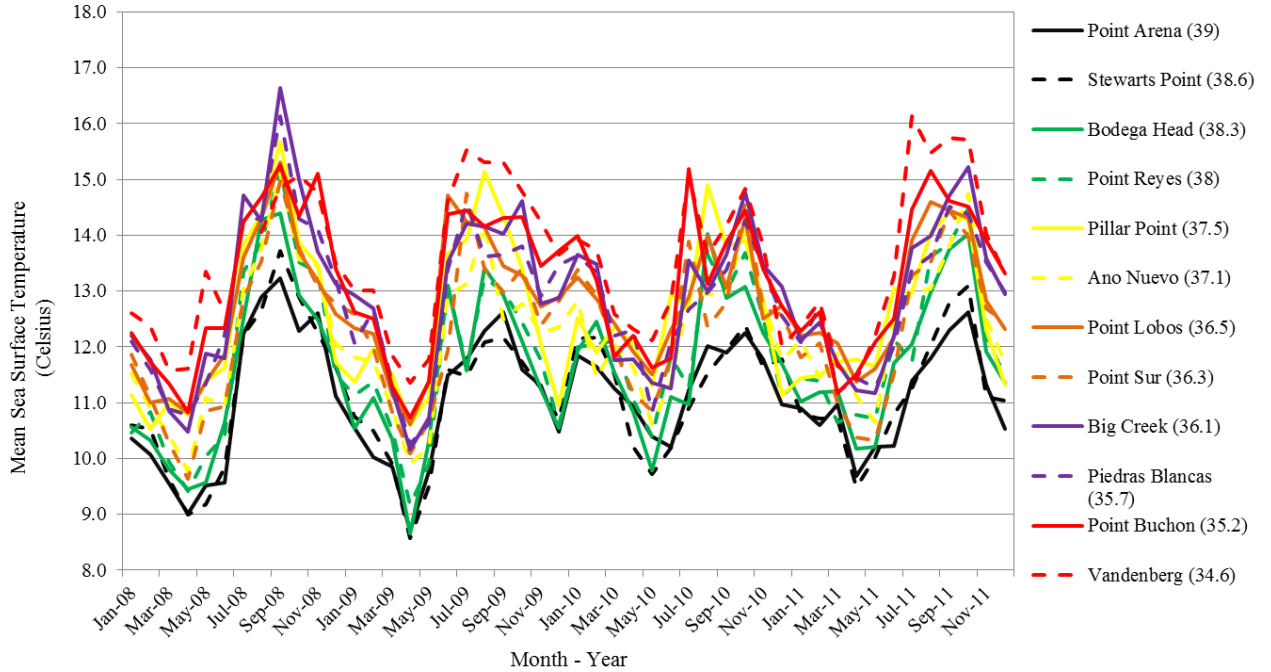


Figure 7: Monthly mean SST for selected MPAs along the central and north-central California coast. The Cambria MPA was excluded due to its relatively small size. Latitude in decimal degrees North are associated with each MPA region.

Fronts

The resulting outputs from the front-finding analysis depended heavily on the parameters input to the tool. The input raster image used for the analysis was the monthly average for April 2009 (cell size 1.3-km). This period corresponds to the annual low for 2009 and assumes peak upwelling (figure 7, above). This analysis observed the results from adjusting the following algorithm parameter inputs: front detection threshold (ΔTemp), histogram window size, histogram window stride, and filter window size (table 1). Single and global population cohesion were recalculated as a function of window size (Roberts et al. 2010):

$$\text{Single Population Cohesion} = 1 - 0.02 - \left(\frac{1}{\text{size}_{\text{window}}} \right) - 2(\alpha)$$

$$\text{Global Population Cohesion} = 1 - \left(\frac{1}{\text{size}_{\text{window}}} \right) - 2(\alpha)$$

Single and global population cohesion respectively check for homogeneity within individual water masses and heterogeneity between water masses within the histogram window. Lower cohesion values permit ‘fuzzier’ boundary regions to be returned in the output as fronts. α corresponds to the probability of falsely identifying a front. For this analysis $\alpha = 0.05$.

Table 1: Input parameters for identifying sea surface temperature fronts using the Cayula and Cornillon Find Fronts Tool in Marine Geospatial Ecology Toolbox.

Trial	Δ Temp ($^{\circ}$ C)	Window Size (#cells)	Window Stride (#cells)	Filter size (#cells)	Local Cohesion	Global Cohesion
1	0.5/1.0	32	16	3	0.9	0.92
2	0.5/1.0	100	50	3	0.87	0.89
3	0.5/1.0	100	20	3	0.87	0.89
4	0.5/1.0	100	20	15	0.87	0.89

Other algorithm input parameters (proportion of pixels with data (0.65), proportion of smaller population (0.25), criterion function value (0.76)) were kept as default for this analysis. The tool does not recommend altering the population proportion or criterion function value. The proportion of pixels parameter is the minimum proportion of cells within the histogram window to contain data in order for the algorithm to execute. This parameter would have an effect on the edges of the image, such as along the shoreline.

The first trial kept default inputs for all parameters and identified the minimum temperature gradient threshold as 0.5° C (left) and 1.0° C (right) (figure 8). This iteration identified fronts between two water masses, which differ by either 0.5° C or 1.0° C, within a 32 x 32 cell (41.5 x 41.5-km) window. As expected, the lower threshold identified more fronts in the SST raster. Increasing the threshold constrains the results to larger gradients, however if those gradients do not exist in nature or within the input window, then the results will be limited.

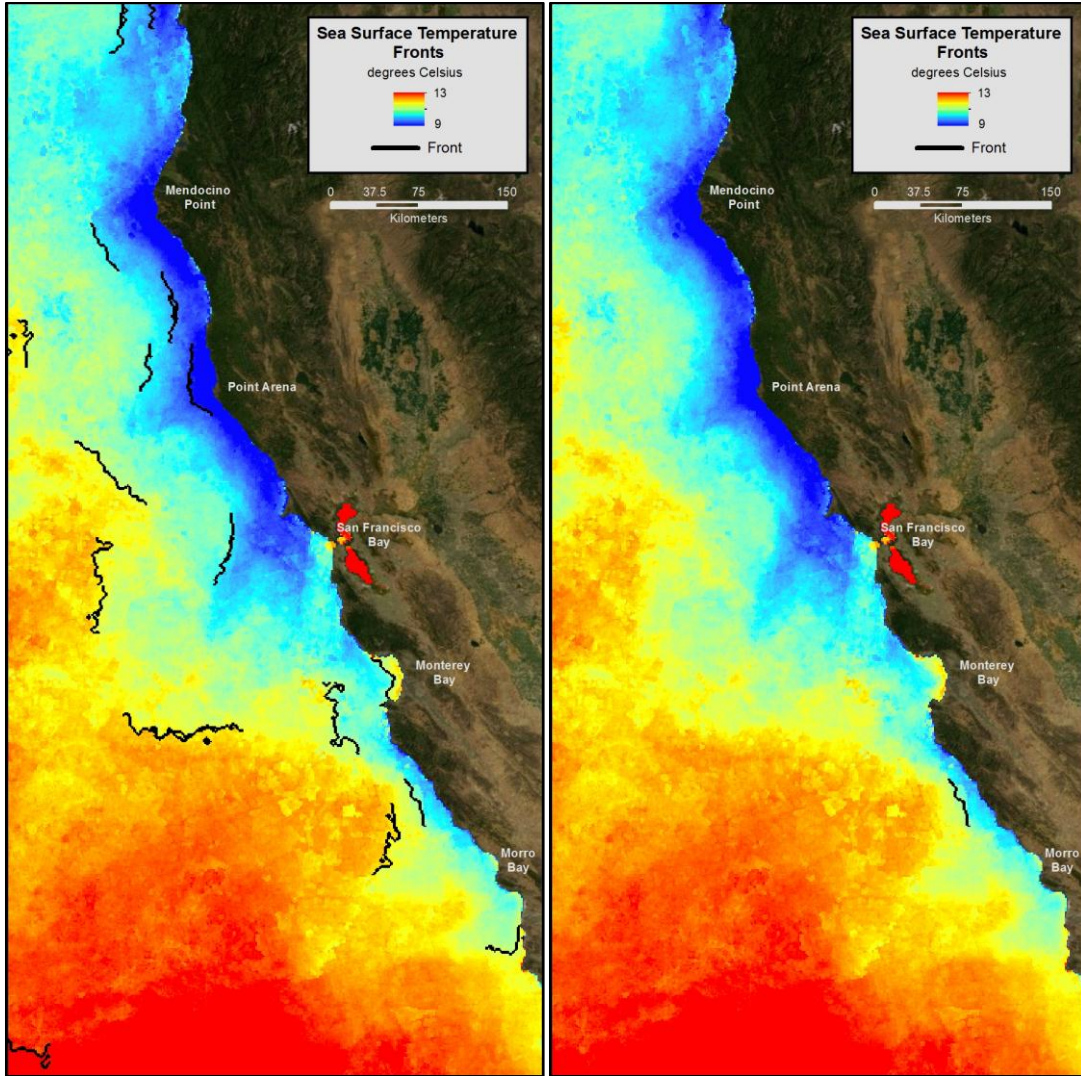


Figure 8: Front analysis with differing gradient thresholds. Left pane computed with a 0.5°C gradient, right pane computed with a 1.0°C gradient. All other input parameters are equal and kept as the tool's default values. SST measurements are April 2009 average (1 cell = 1.3km).

The second trial kept the same gradient thresholds of 0.5°C (left) and 1.0°C (right) and increased the histogram window to 100 x 100 cells (130 x 130 km). The single and global population cohesion's were recalculated to reflect this change. Window stride, the number of cells the window jumps between algorithm runs, was increased to 50 cells. Increasing the window stride to one-half the window size mimicked the convention Robertson et al. (2010) portrayed in the tool's default settings. This method instructs the window to construct a histogram with 50% new data with each jump. Higher values reduce the number of redundant front observations, however they can also cause fronts to

be missed. This trial identified several 0.5°C gradients and no 1.0°C gradients (figure 9). Although the window had a broader extent than the previous trial, this trial's output produced fewer fronts. In addition to the increased stride, this result could be explained by the population proportion parameter. This parameter evaluates the relative size of the distinct water masses and only identifies a front when the smaller water mass (within the window) exceeds the indicated value. By default, an individual water mass must be encompassed by a minimum of 25% of the cells in the histogram window in order to be recognized by the algorithm. Therefore, with a larger window making longer strides, homogenous water masses must be spatially large in order to be recognized by the tool. As a result, the cold water mass near Mendocino Point and Point Arena may have been missed.

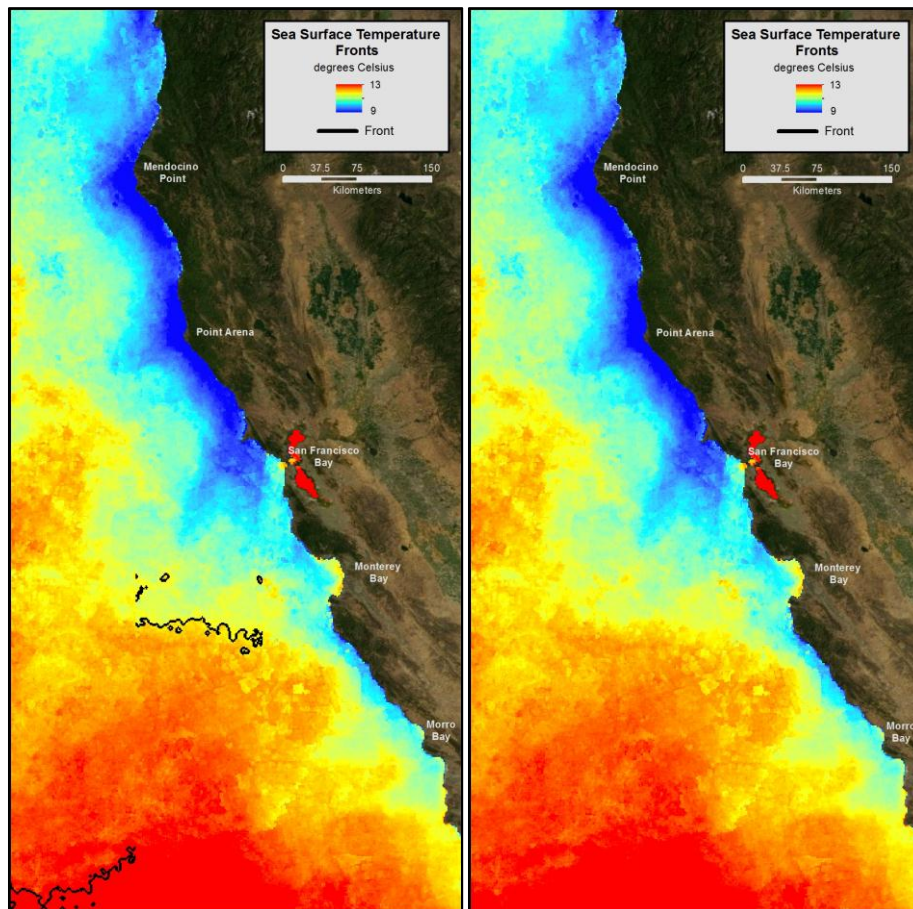


Figure 9: Front analysis identifying differing temperature gradients within a 100×100 cell window on a 50 cell stride. Left pane identified 0.5°C gradients, right pane identified 1.0°C gradients. All other input parameters are equal. SST measurements are April 2009 average (1 cell = 1.3km).

The third trial kept the same parameters as the previous trial, but reduced the stride to 20 cells (26-km). As expected, the shorter stride identified more fronts throughout the image (figure 10). In both cases (0.5 and 1.0 °C thresholds) a front is delineated between the cold upwelled coastal water along the north central coast and the warmer offshore water. The lower gradient threshold of 0.5°C (figure 8, left) also identified several fronts further offshore.

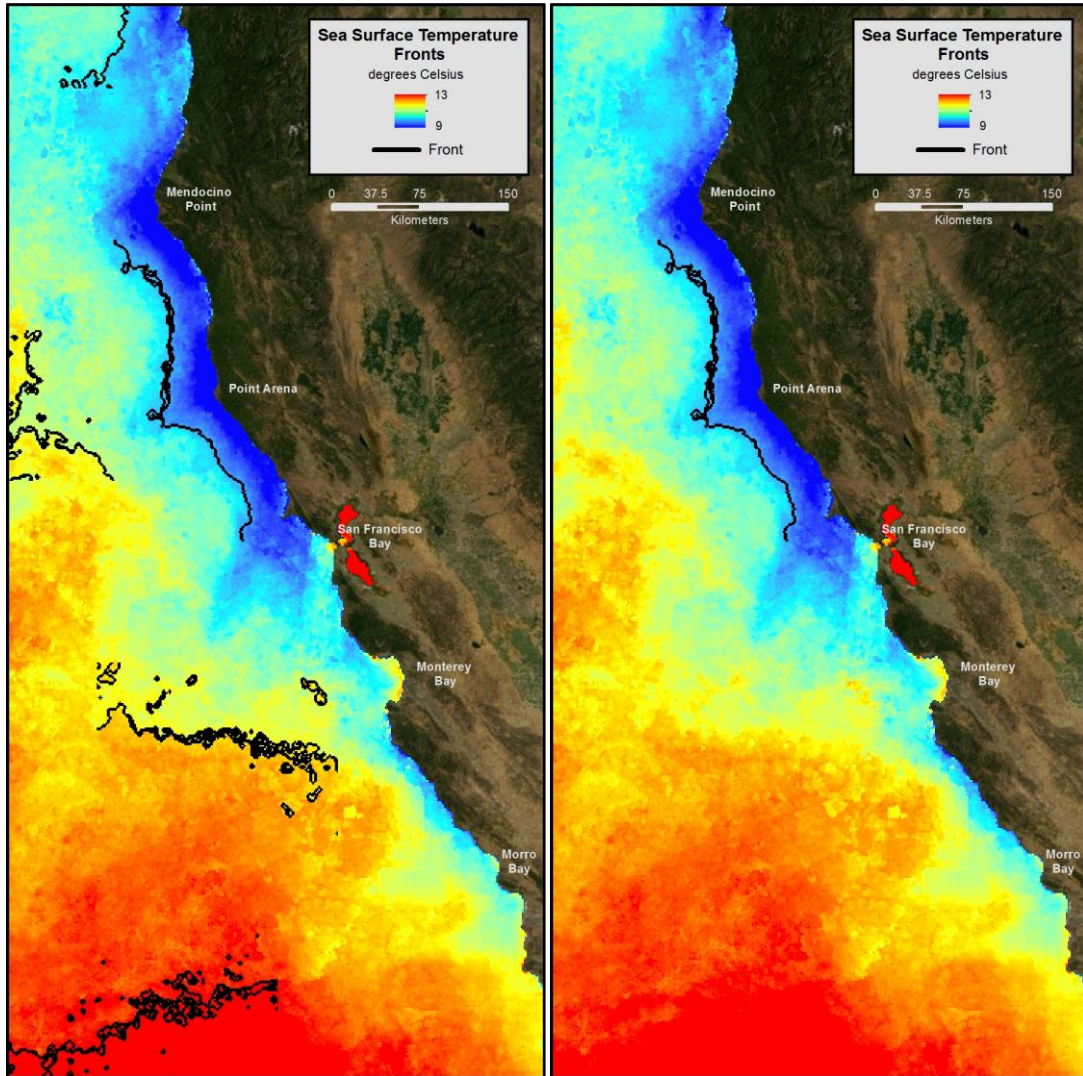


Figure 10: Front analysis with a 20 cell histogram window stride. Left pane computed with a 0.5°C or more temperature difference, right pane computed with a 1.0°C or more temperature difference. All other input parameters are equal. SST measurements are April 2009 average (1 cell = 1.3km).

The final trial focused on adjusting the filter window size. Prior to running the algorithm, a moving filter window smooths out the data in the raster image. The size of

the window determines how coarsely the image is filtered. The default filter window is 3 x 3 cells, which is the size used in the first three trials. For this trial the window size was increased to 15 x 15 cells. As expected, lines designating the fronts were smoothed when compared to the previous trial (figure 11). This gives the fronts a cleaner, more streamlined appearance; which is more aesthetically pleasing for visualizations. Smoothing the data also resulted in identifying several additional gradients throughout the image.

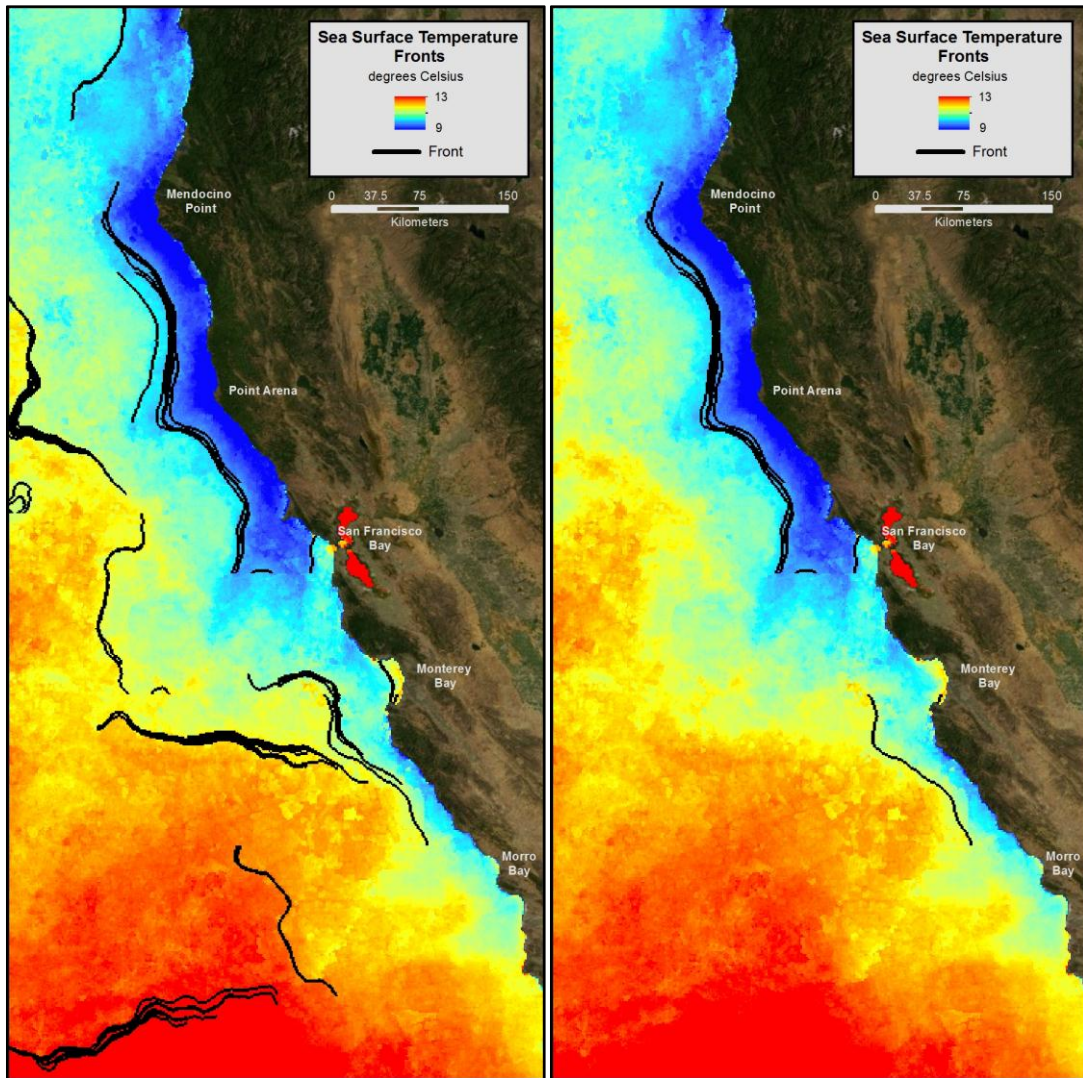


Figure 11: Front analysis with a 15 x 15 cell filter window. Left pane computed with a 0.5°C or more temperature difference, right pane computed with a 1.0°C or more temperature difference. All other input parameters are equal. SST measurements are April 2009 average (1 cell = 1.3km).

DISCUSSION

This project demonstrates that some dynamic properties of the marine environment can be analyzed and visualized with geospatial software. Time series of spatially averaged sea surface temperature (SST), as well as along-shore and cross-shore current, were plotted for selected marine protected areas (MPAs) along the central and north-central California coast. Furthermore, an open-source tool was used to identify temperature fronts and delineate upwelling regions. Raster data layers accessible through geographic information systems (GIS) software enabled these types of analyses. Creating oceanographic datasets, such as SST, chlorophyll, currents, and wind, executable in GIS software could potentially expand their incorporation into California marine management decisions.

California's MPA network was designed to conserve ecosystem integrity within the state's subtidal region (MLPA 2004). Monitoring efforts are underway to evaluate the changing conditions of state marine ecosystems (MPA Monitoring Enterprise 2011). One concern is the impact climate change will have on temperate marine ecosystems (Score et al. 2011). Rising sea temperatures and changes in atmospheric conditions could have profound influences on marine biological communities (Doney et al. 2012, Hayward 1997). Changing sea temperatures may induce shifts in species distributions or enhance conditions for non-native species recruitment (Doney et al. 2012). Similarly, a warming planet can drive changes in wind patterns causing unknown variability in ocean surface currents (Schwing et al. 2010). This variability could impact seasonal upwelling and larval transport (Song et al. 2011, Kimura et al. 2010). Maintaining up-to-date time series of oceanographic parameters, such as those detailed in this project, with respect to MPA boundaries could capture gradual changes in ocean conditions. This could assist marine managers in making informed decisions on how to protect and conserve marine ecosystems.

Offering oceanographic datasets in GIS formats will broaden marine research capabilities. ArcGIS software has already proven to be a powerful geostatistical tool for many marine researchers. ArcGIS has been used in pollution impact monitoring, species habitat modeling, and marine spatial planning (Baguley (seminar), Young et al. 2010,

UCSB 2012). Furthermore, ESRI, the creator of ArcGIS, has been expanding its marine GIS processing and visualization capabilities to enhance marine research and management (Wright 2012). The most commonly used datasets for marine research and management purposes are multibeam bathymetry, and a wide range of data types to represent political boundaries, sampling locations, or static environmental features (e.g. rocky habitat). While these data are very important in marine research and management, they are not the whole picture. More temporally variable oceanographic parameters have largely been absent from these geospatial ecological and marine spatial planning analyses and depictions. Incorporating dynamic oceanographic datasets into ArcGIS formats would allow for more comprehensive marine research at local to global scales, for improving our understanding of marine processes, interactions, and impacts.

As oceanographic and atmospheric numerical model output and remotely-sensed, and especially in-situ, observations continue to achieve finer spatial resolution, the opportunities for integrated analyses and depictions of oceanographic, ecological, and political boundary datasets will increase. Our ability to manipulate these oceanographic product datasets must also increase. Geospatial software, such as ArcMap, is one data processing tool that is widely used by marine researchers and managers. Therefore, providing oceanographic datasets in formats that are executable with ArcGIS software could expand research and visualization capabilities.

ACKNOWLEDGEMENTS

Funding Sources: NOAA Grant #NA11NOS0120032 and MBARI. Data Sources: NOAA CoastWatch ERDDAP, Scripps Institution of Oceanography Coastal Observing Research and Development Center, Naval Research Laboratory-Monterey. Project assistance: Leslie Rosenfeld (CeNCOOS), Fred Bahr (CeNCOOS), Rikk Kvitek (CSU Monterey Bay Seafloor Mapping Lab), Pat Iampietro (CSU Monterey Bay Seafloor Mapping Lab), Madhavi Colton (California Ocean Science Trust), Jennifer Patterson (CeNCOOS), Scott Hamilton (Moss Landing Marine Laboratories), Monique Messié (MBARI), Dave Foley (NOAA), Jason Roberts (Duke University).

References:

Anderson TJ, Cymys C, Roberts DA, Howard DF (2009). Multi-scale fish-habitat associations and the use of habitat surrogates to predict the organization and abundance of deep-water fish assemblages. *Journal of Experimental Marine Biology and Ecology* 379: 34-42.

Baguley, Jeff. Deep sea benthos response to the Deepwater Horizon oil spill. Monterey Bay Aquarium Research Institute [Organization]. Moss Landing, CA. 08 August 2012.

Cayula J, Cornillon P (1992). Edge detection algorithm for SST images. *Journal of Atmospheric and Oceanic Technology* 9: 67-80.

[CDFG] California Department of Fish and Game (2012). Downloads: Marine Region GIS Unit [Internet]. [Cited 1 October 2012]. Available from: <http://www.dfg.ca.gov/marine/gis/downloads.asp>.

Crowder L, Norse E (2008). Essential ecological insights for marine ecosystem-based management and marine spatial planning. *Marine Policy* 32(5): 772-778.

Dawe JT, Thompson L (2006). Effect of ocean surface currents on wind stress, heat flux, and wind power input to the ocean. *Geophysical Research Letters* 33(9): 1-5.

Doney SC, Ruckelshaus M, Duffy JE, Barry JP, Chan F, English CA, Galindo HM, Grebmeier JM, Hollowed AB, Knowlton N, Polovina J, Rabalais NN, Sydeman WJ, Talley LD (2012). Climate change impacts on marine ecosystems. *Annual Review of Marine Science* 4: 11-37.

[ESRI] Environmental Systems Resource Institute 2011. ArcGIS Desktop: Release 10. Redlands, CA: Environmental Systems Research Institute.

Hayward T (1997). Pacific Ocean climate change, atmospheric forcing, ocean circulation and ecosystem response. *Trends in Ecology and Evolution* 12(4): 150-154.

Kahru M, Kudela RM, Manzano-Sarabia M, Mitchell BG (in press). Trends in the surface chlorophyll of the California current: merging data from multiple ocean color satellites. *Deep-Sea Research II*.

Kim SY, Terrill E, Cornuelle B (2007). Objectively mapping HF radar-derived surface current data using measured and idealized data covariance matrices. *Journal of Geophysical Research* 112: 1-16.

Kim SY, Terrill EJ, Cornuelle BD (2007). Objectively mapping HF radar-derived current data using measured and idealized data covariance matrices. *Journal of Geophysical Research* 112, C06021, doi: 10.1029/2006JC003756.

Kim SY, Terrill EJ, Cornuelle BD (2008). Mapping surface currents from HF radar radial velocity measurements using optimal interpolation. *Journal of Geophysical Research* 113, C10023, doi: 10.1029/2007JC004244.

Kim SY (2009). Coastal ocean studies in southern San Diego using high-frequency radar derived surface currents [Doctorate Dissertation]. University of California, San Diego.

Kim SY (2010). Observations of submesoscale eddies using high-frequency radar-derived kinematic and dynamic quantities. *Continental Shelf Research* 30: 1639-1655.

Kimura S, Kato Y, Kitagawa T, Yamaoka N (2010). Impacts of environmental variability and global warming scenario on Pacific bluefin tuna (*Thunnus orientalis*) spawning grounds and recruitment habitat. *Progress in Oceanography* 86: 39-44.

Kirwan II AD (1985). A review of mixture theory with applications in physical oceanography and meteorology. *Journal of Geophysical Research* 90(C2): 3265-3268.

Leegard KR, Thomas AC (2006). Spatial patterns in seasonal and interannual variability of chlorophyll and sea surface temperature in the California current. *Journal of Geophysical Research* 111: 1-21.

Leslie HM, McLeod KL (2007). Confronting the challenges of implementing marine ecosystem-based management. *Frontiers in Ecology and the Environment* 5(10): 540-548.

MacCall AD, Prager MH (1988). Historical changes in abundance of six fish species off southern California, based on CalCOFI egg and larva samples. *Reports of California Cooperative Oceanic Fisheries Investigations* 29: 91-101.

MATLAB version 7.14.0. Natick, Massachusetts: The MathWorks Inc., 2012.

[MLPA] Marine Life Protection Act. Fish and Game Code, Section 2851(f). Amended to July 2004. Available from: http://www.dfg.ca.gov/mlpa/pdfs/mlpa_language.pdf.

MPA Monitoring Enterprise (2011). Implementing monitoring [Internet]. [Cited 27 August 2012]. Available from: <http://monitoringenterprise.org/role/implementing.php>.

[NASA] National Aeronautics and Space Administration (2011). MODIS Web: about MODIS [Internet]. [Cited 16 August 2012]. Available from: <http://modis.gsfc.nasa.gov/about/>.

[NRL] Naval Research Laboratory (2003). COAMPS version 3 model description: general theory and equations (NRL/PU/7500—03-448). Naval Research Laboratory: Marine Meteorological Division, Monterey, CA.

O'Reilly JE, Mueller JL, Mitchell BG, Kahru M, Chavez FP, Strutton P, Cota GF, Hooker SB, McClain CR, Carder KL, Muller-Karger F, Harding L, Magnuson A, Phinney D, Moore GF, Aiken J, Arrigo KR, Letelier R, Culver M (2000). Ocean color chlorophyll a algorithms for SeaWiFS, OC2, and OC4: Version 4. In: SeaWiFS Postlaunch Technical Report Series, edited by Hooker SB, Fireston ER. Volume 11: SeaWiFS Postlaunch Calibration and Validation Analysis, Part 3. NASA, Goddard Space Flight Center, Greenbelt, MD. 9-23.

Roberts JJ, Best BD, Dunn DC, Treml EA, Halpin PN (2010). Marine geospatial ecology tools: an integrated framework for ecological geoprocessing with ArcGIS, Python, R, MATLAB, and C++. *Environmental Modelling & Software* 25: 1197-1207.

Schwarz JN, Raymond B, Williams GD, Pasquer B, Marsland SJ, Gorton RJ (2010). Biophysical coupling in remotely-sensed wind stress, sea surface temperature, sea ice and chlorophyll concentrations in the South Indian Ocean. *Deep-Sea Research II* 57:701-722.

Schwing FB, Mendelssohn R, Bograd SJ, Overland JE, Wang M, Ito S (2010). Climate change, teleconnection patterns, and regional processes forcing marine populations in the Pacific. *Journal of Marine Systems* 79: 245-257.

Score A, Gregg RM, Hansen LJ (2011). Monitoring climate change effects in temperate marine ecosystems. EcoAdapt Technical Report. Bainbridge, WA. Available from:

http://monitoringenterprise.org/pdf/Monitoring_climate_change_effects_in_temperate_marine_ecosystems.pdf.

Shulman I, Wu CR, Lewis JK, Paduan JD, Rosenfeld LK, Kindle JC, Ramp SR, Collins CA (2002). High resolution modeling and data assimilation in the Monterey Bay area. *Continental Shelf Research* 22: 1129-1151.

Song H, Miller AJ, Cornuelle BD, DiLorenzo E (2011). Changes in upwelling and its water sources in the California Current System driven by different wind forcing. *Dynamics of Atmospheres and Oceans* 52: 170-191.

Tchoukanski I (2012). Easy Calculate 10 Tool. Created by ET Spatial Techniques. Available from: <http://www.ian-ko.com/>.

[UCSB] University of California Santa Barbara (2012). McClintock Lab: SeaSketch [Internet]. [Cited 28 August 2012]. Available from: <http://mcclintock.msi.ucsb.edu/projects/seasketch>.

Walton CC, Pichel WG, Sapper JF, May DA (1998). The development and operational application of nonlinear algorithms for the measurement of sea surface temperatures with the NOAA polar-orbiting environmental satellites. *Journal of Geophysical Research* 103(C12): 27999-28012.

Wright D (2012). The ocean GIS initiative: ESRI's commitment to understanding our oceans [ebook]. [Cited 28 August 2012]. Available from: <http://www.esri.com/library/ebooks/ocean-gis-initiative.pdf>.

Young MA, Iampietro PJ, Kvitek RG, Garza CD (2010). Multivariate bathymetry-derived generalization linear model accurately predicts rockfish distribution on Cordell Bank, California, USA. *Marine Ecological Progress Series* 415: 359-371.

APPENDIX A

File Parameter Conversion Workflow

SST and Chlorophyll

This workflow details the steps taken to download SST and Chlorophyll observations from the NOAA CoastWatch ERDDAP (<http://coastwatch.pfeg.noaa.gov/erddap/griddap/index.html?page=1&itemsPerPage=1000>) and convert it to ARC GRID raster format (Figure 1).

- 1. Get the raw data from CoastWatch:** This originally started with a MATLAB script created to pull 3-day composited SST data from the CoastWatch GRIDDAP based on a defined time period. The script asks the user to specify a year and quarter of data to download. The grid extents were defined as 32.5 to 42 degrees Latitude and 234 to 243 degrees Longitude. This script creates a 3-dimensional array with X/Y corresponding to the data at each Lon/Lat and Z representing each 3-day composite. Separate Lat (*lat1*), Lon (*lon1*), and time (*time*) arrays are created to reference the data. This code was also modified to download 3-day composited chlorophyll data.

To speed up this process I created a simple looping script that automatically inputs the date ranges into the above script. With this script I was able to download the full dataset with one run of the script.

Outputs: the raw outputs of this step are quarterly MAT files containing measurement arrays (*Tarr/Chlarr*), Latitude array (*lat1*), Longitude array (*lon1*), and a time array (*time*).

- 2. Convert to ASCII file:** The function (*arcgridwrite.m*) from the MATLAB File Exchange converted the observation arrays into ASCII text files. This function takes 4 inputs: output file name, Longitude (*X*), Latitude (*Y*), observation (*Z*). The function examines the grid cell spacing in the X and Y variables and throws an error if $dX \neq dY$. If you pass without errors the function will write an ASCII file for each day within the *Tarr/Chlarr* array.

To speed up this process I created a simple looping script that will open and convert each of the quarterly MAT files (created from the previous step) for a year.

Output: daily 3-day composited ASCII text files.

- 3. Convert to ARC GRID Rasters:** The final step was performed in ArcMap. I created a tool (*ASCII converter*) that converts an ASCII file into a georeferenced

ARC GRID Raster layer. The tool essentially iterates through a list of ASCII files in a folder and goes through the process of converting it into a raster (ASCII to Raster tool), clipping that raster at the shoreline (to eliminate measurement of lakes), defines the coordinate system as WGS 1984, and projects the raster to NAD 1983 California Teale-Albers. A raster must be projected in order for spatial statistics to be successful. I selected NAD83 CA Teale-Albers because the SST/Chlorophyll measurements cover the whole length of CA.

Output: Daily 3-day composited ARC GRID rasters projected into NAD83 CA Teale-Albers.

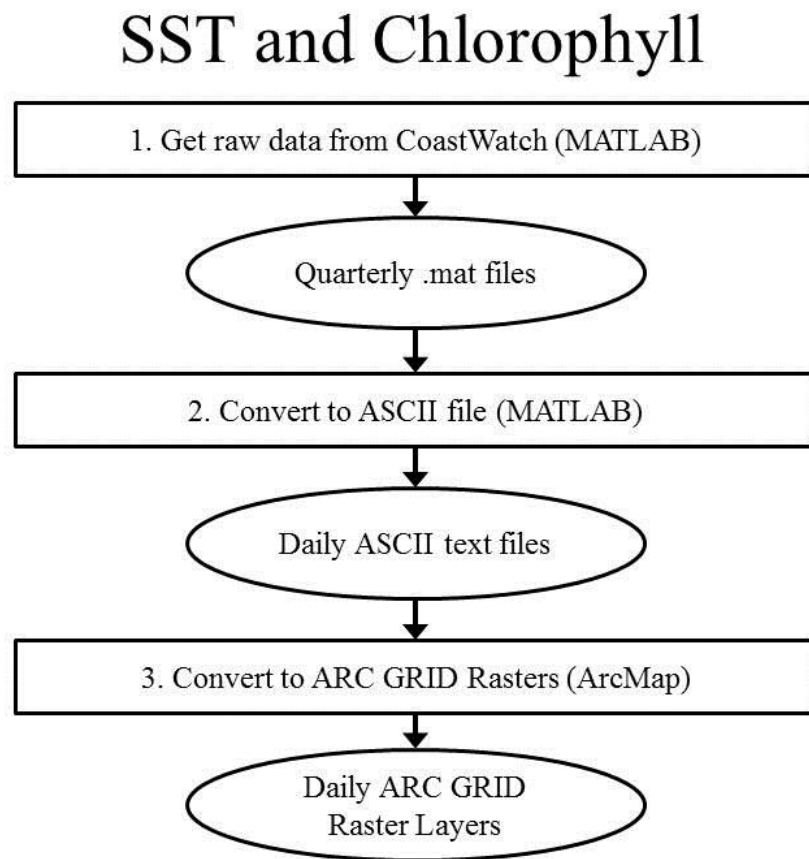


Figure 1: Simple workflow diagram of steps to convert SST and Chlorophyll from source to ARC GRID format.

HF Radar

This section provides the workflow I used to create the HF radar u and v raster data (Figure 2). The HF Radar files were provided by Dr. Sung Yong Kim from the Scripps Institution of Oceanography Coastal Observing Research and Development Center. The original HF radar MAT files I received were too large to open both the PC and Linux machines. Therefore, I had to add a couple extra steps of processing to get the job done. It was good experience for me, but surely there is a more elegant way of computing.

- 1. Separate annual files into quarterly files:** the original data files provided were the truncated-to-California hourly HF data for each full year of 2008 and 2009. The data consisted of grid arrays (*LatU/LonU*), a grid/data reference array (*mylist*), u and v 3D data arrays (*u2008* and *v2008*), and a time array (*t2008*). Attempts to open the MAT files on both the PC and Linux shell incurred the ‘Out of Memory’ error. After consulting with other MATLAB users, I decided to break up the annual data and save them into quarterly MAT files.

Output: Quarterly MAT files containing only lat/lon grid, reference list, and hourly u, v, and time arrays.

- 2. A. Average hourly measurements into 3-day composites:** To stay consistent with the SST/Chlorophyll data, I chose to average the HF radar data to the same 3-day composites; wherein a particular day is averaged with the full day before and full day after. To achieve this I found a function on the MATLAB File Exchange that runs a moving average on the data (*movavgFilt.m*). This function takes 3 inputs: the input dataset to be averaged (*In*), the length of the averaging window (*Len*), and a string to indicate the averaging method (*Left*, *Right*, or *Center*). The input datasets were 3-dimensional with the hourly observations along the z-axis. The data were averaged along the z-axis. I created a simple code that runs this moving average and generates outputs (*u_mean* and *v_mean*). I used a 73-hour window around the ‘Center’ observation. A 73-hour window was used because an even number was not allowed for the ‘Center’ option.

Because this function averages every single hour in the data, I needed to pull out the data points that I wanted to keep. So I pulled out every 24th hour of the data, beginning with the 13th hour (12noon on the first day) and saved them as *ucomp* and *vcomp*. The same was done for the time component (*tcomp*).

- 2. B. Calculate 3-day composites for beginning and end dates of each quarter:** Because the data were broken up into quarters prior to averaging, the first and last days of each quarter would not have been averaged correctly using the 73-hour window. So I created a script that extracts date ranges from the original, annual data and calculates new 73-hour means from those ranges. For example in Q1 and Q2, March 31st and April 1st were in separate files and thus were not averaged

together. The script extracts the hourly observations from March 30th through April 2nd from the original data and computes new 73-hour averages for March 31st and April 1st. The new averages for the beginning and end of each quarter replaced the respective previous daily averages computed in step 2a. January 1st, 2008 and December 31st, 2009 are averages of the target date and respectively the day after and day before.

Output: quarterly MAT files of 3-day composites of HF u and v data. *ucomp* and *vcomp* are the actual 3-day composites.

- 3. Convert to Geotiff:** several attempts of writing the u and v data into ASCII using the *arcgridwrite.m* function consistently returned errors regarding the lat/lon grid cell spacing, indicating the grid cells were not square. To reconcile this problem I wrote the data to a geotiff file format using the *geotiffwrite* function in the MATLAB Mapping Toolbox. Geotiffwrite takes 3 inputs: output file name, input data, and a worldfile (*R*). The worldfile is a structure file that contains georeferencing information. The user can define lat/lon extents and grid cell spacing. See *spatialref.GeoRasterReference* in MATLAB help.

Output: I created a script to convert each 3-day composite for each quarter into geotiff raster images.

- 4. Convert to ARC GRID:** Geotiff u and v rasters were acting rather problematic and clunky in ArcMap, so they were converted to ARC GRID format. I created a model (Geotiff Converter) to do this operation. The model iterates through each geotiff in a folder, calculates statistics, copies it into ARC GRID format, defines a coordinate system, and projects it to NAD 83 CA Teale-Albers.

Output: 3-day composites of u and v raster images in ARC GRID format.

HF Radar

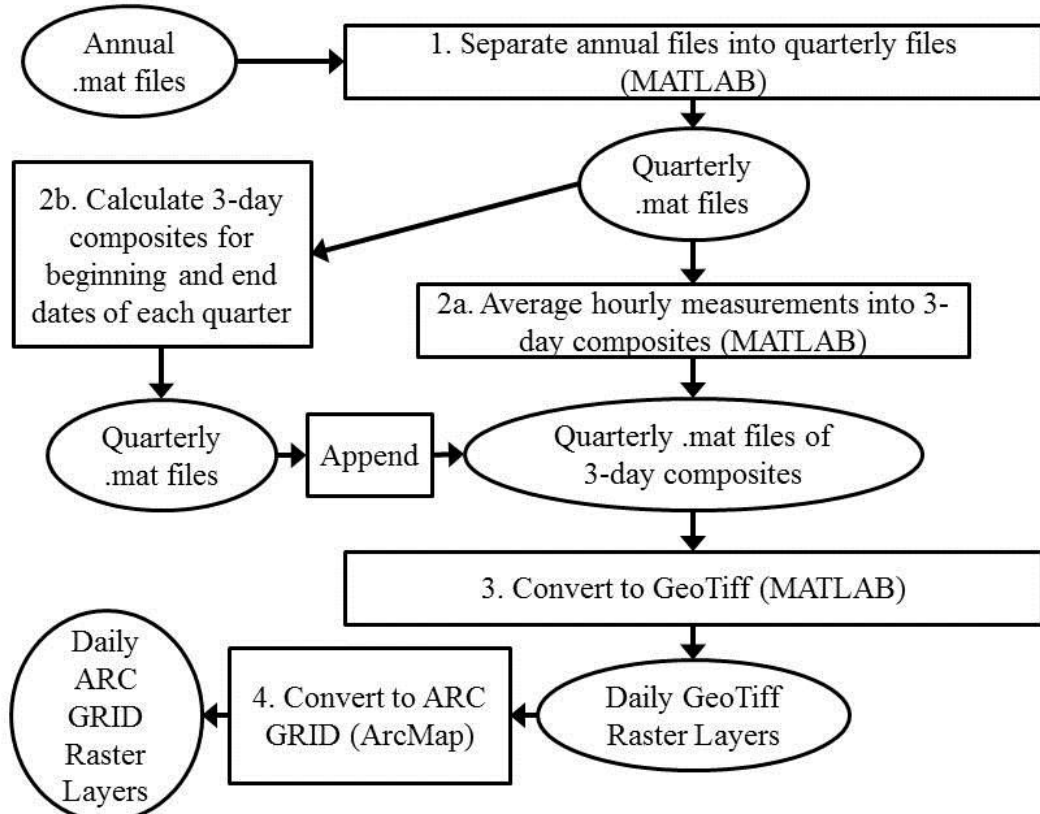


Figure 2: Simple workflow diagram of steps to convert HF Radar data from source to ARC GRID format.

COAMPS Wind

This section provides the workflow I used to create the COAMPS wind *u* and *v* raster images (Figure 3). The data were provided to me in a series of Tarr archive files by the Naval Research Laboratory in Monterey. The data can also be accessed from the US Global Ocean Data Assimilation Experiment server (<http://www.usgodae.org/cgi-bin/datalist.pl?generate=summary>).

1. **Extract data from Tarr files:** I modified a pre-existing code provided that unpacks Tarr files and save them as MAT files. There is a different Tarr file for every 12 hours from April 14th, 2009 at 12pm to May 31st, 2012 at 12pm. Each Tarr file contains a nowcast, plus 48 hourly forecasts. For each Tarr file, the code opens the archive, extracts the nowcast and first 12 hourly forecasts, averages those measurements together, and saves those averages (*uwind* and *vwind*) into a new MAT file. If a Tarr file for a particular time did not exist, which happened several times throughout the dataset, the code jumped back 24 hours to a prior Tarr file and averaged the 24th through 35th forecasted hours.

Output: MAT files of wind vector components averaged over 12 hours, occurring on a frequency of 12 hours.

2. **Compile wind measurements for averaging:** To stay consistent with the other datasets, the wind dataset was also averaged to a 3-day composite. To achieve this I created a code that opens each 12pm MAT file, as well as the 3 MAT files prior and 2 after, and compiles the measurements into the 12pm MAT file. Essentially, the code is grabbing the 36 hours prior (*obs12*, *obs24*, *obs36*) to the 12pm measurement (*obs*), which is the average from 12pm to midnight, and finally the 24 hours of the next day (*obs_12*, *obs_24*). If one of those averages did not exist, an array of NaNs was created as a place holder.

Output: MAT files of wind vector components ready for averaging to 3-day composites, occurring on a frequency of 12 hours.

3. **Average components to 3-day composites:** With a new script, each file was opened and the observations within them were concatenated into a 3D array. The 3D array was averaged with the *nanmean.m* function, which ignores any NaNs in the data.

Output: 3-day composites of wind vector data (*uwind*, *vwind*), saved as *YYYYMMDDHH_windmean.mat*.

4. **Rotate averaged components to true coordinate system:** this step computes new vector components (*utru*, *vtru*) based on a grid that is slightly rotated

(*gridrot*). Gridrot is an array of vector rotation multipliers created to project the wind vector components from a standard longitude to true longitude.

Output: new vector components (*utru, vtru*) saved in the existing MAT file.

- 5. Interpolate measurements onto mesh-grid:** first attempts to write the vector component measurements to and ASCII or geotiff resulted in the final raster layer not properly aligning with the CA coastline. This was due to the variably grid cell sizing of the lat/lon grid. Therefore the measurements were interpolated onto a new grid with square cells and matched with a new mesh grid coordinate system.

Output: *new_u* and *new_v* saved in the existing MAT file.

- 6. Export to ASCII file:** similar to step 2 in SST/chlorophyll flowchart

- 7. Convert to ARC GRID:** similar to step 3 in SST/chlorophyll flowchart. A different model was created for this process (*ASCII Wind Converter*).

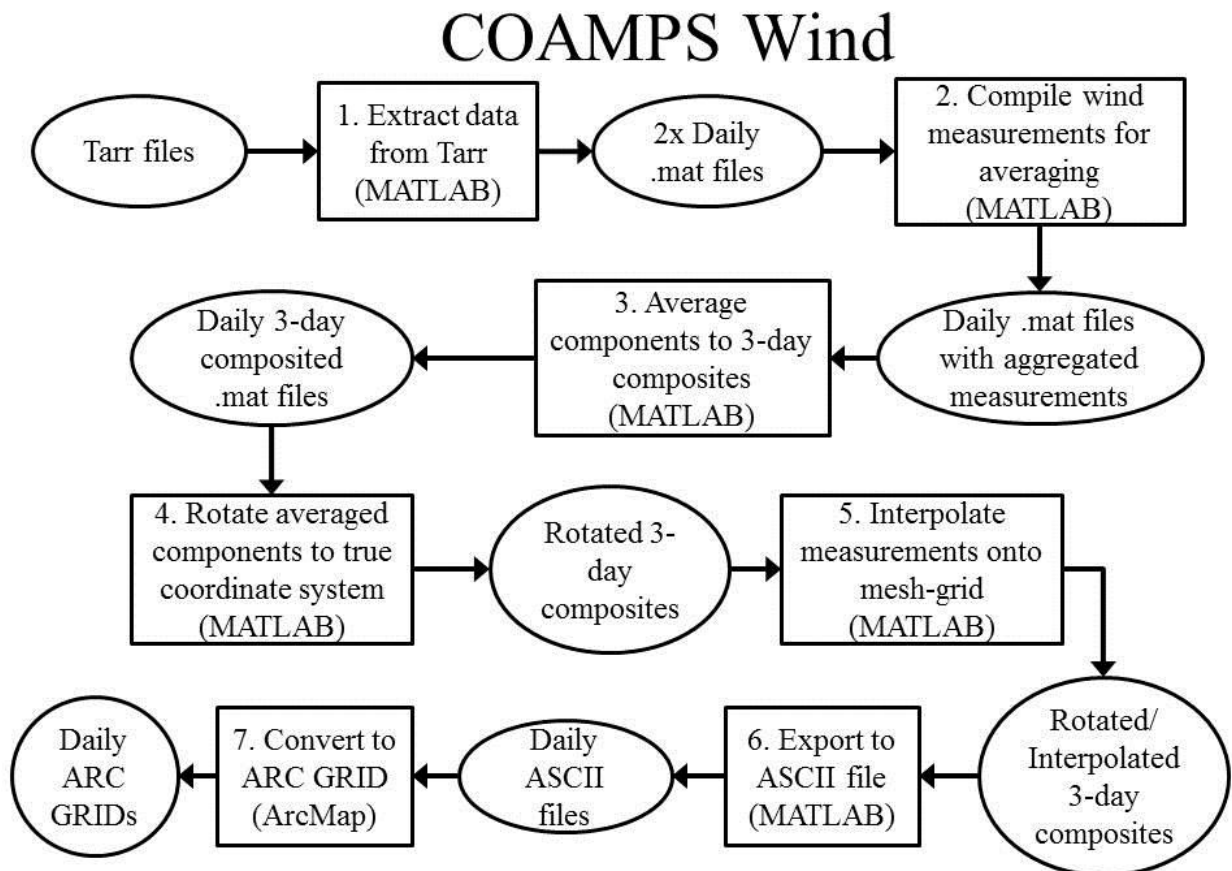


Figure 3: Simple workflow diagram of steps to convert COAMPS wind data from source to ARC GRID format.